FACTA UNIVERSITATIS
Series: **Automatic Control and Robotics** Vol. 16, N° 3, 2017, pp. 229 - 240
https://doi.org/10.22190/FUACR1703229G

CPML PARAMETER OPTIMIZATION IN FDTD MODELING OF IMPULSIVE SOURCE

UDC ((537.8+539.4.011):519.6)

Branko Gvozdić[1], Dušan Đurđević[1], Nebojša Raičević[2]

[1]University of Priština, Faculty of Technical Sciences, Kosovska Mitrovica, Republic of Serbia
[2]University of Niš, Faculty of Electronic Engineering, Niš, Republic of Serbia

Abstract. *The convolutional perfectly matched layer (CPML) is currently, perhaps, the most efficient type of absorbing boundary condition in finite difference time domain method (FDTD) modeling of electromagnetic fields. The aim of this paper is to give a more detailed insight into parameter setting and absorption performance of CPML. In case of electromagnetic waves absorption for high-frequency impulsive source modeling, a proper choice of the CPML parameters is substantial. The numerical results show that stretching coefficient affects both absorption efficiency and dispersion. We demonstrate that, in order to eliminate dispersion, the stretching coefficient should be as small as possible. Additionally, the results have shown that a differentiated Gaussian pulse is a better choice than a regular Gaussian pulse in FDTD simulations.*

Keywords: *finite difference time domain, FDTD, perfectly matched layer, PML, convolutional PML, CPML parameters*

1. INTRODUCTION

One of the most popular numerical methods in computational electromagnetics (CEM) is finite difference time domain (FDTD) method. FDTD method is commonly used for simulation of electromagnetic wave propagation and interaction with complex and largely inhomogeneous structures. FDTD computer simulations are often used to simulate electromagnetic field propagation of antenna radiation, to calculate radar cross-section, and in microwave and photonics design.

Absorbing boundary conditions (ABC) are implemented at the computational domain boundaries in order to simulate infinite space in FDTD simulations. The perfectly matched layer (PML) [1] is one of the most efficient ABCs. PMLs are used in the absorption of

Received July 15, 2017
Corresponding author: Branko Gvozdić
University of Priština, Faculty of Technical Sciences, Kosovska Mitrovica, Republic of Serbia
E-mail: branko.gvozdic@pr.ac.rs

electromagnetic waves of arbitrary polarization, the angle of incidence and frequency. It is based on non-physical field splitting of Maxwell's equations and it is applicable in homogeneous, inhomogeneous, linear, nonlinear, dispersive and anisotropic domains. Uniaxial PML (UPML) [2] has the same efficiency as the split-field PML [3,4]. Stretched coordinate (SC) formulation of Maxwell's equation extended the use of the PML into other orthogonal coordinate systems [5, 6] and into general curvilinear coordinate systems [7,8]. The usage of complex frequency shifted (CFS) tensor coefficients for PML parameters in [9, 10] gained the causality of PML. Very effective implementation of PML based on SC, CFS and recursive convolution technique [11] is derived in [12]. Convolutional PML (CPML) [12] is entirely independent of the host medium and without the need of any modifications when applied in inhomogeneous, lossless, lossy, dispersive, nonlinear and anisotropic media. Improved CPMLs are recently derived in [13, 14]. Although numerous papers show that CPML is efficient, there is a space for improvement in the case of specific electromagnetic problems. Researches based on the dominant absorption frequency are very common [14,15], however, research regarding optimization of parameter setting has just begun [16].

FDTD method recognizes, in general, different types of electromagnetic sources. Source selection is based on multiple factors: FDTD domain dimension (1D, 2D, 3D space), geometry of computational domain (waveguide, optical fiber, etc.), physical structure of computational domain (free space, half-space, etc.). The most common is the use of pulse sources with Gaussian and sinusoidal base function. Pulse sources of electromagnetic field are characterized with propagation in all directions of computational domain and generation of a wide range of frequencies. Numerous practical electromagnetic problems can be solved by using electromagnetic wave propagation generated from an impulse source.

In our recent paper [17], the advantages of CPML over UPML are investigated. We demonstrated that CPML is a better choice in terms of implementation in FDTD method, electromagnetic wave absorption and the use of computer resources.

In this paper, we focus mainly on improvement of CPML electromagnetic wave absorption using optimisation of CPML parameters. Influence of different CPML parameter settings on the absorption of electromagnetic waves in high-frequency impulsive source modeling is investigated with an extensive number of numerical experiments. Firstly, the use of two different pulse sources in FDTD method is examined and proposal about the choice of the source is given. Subsequently, a 3D FDTD simulation of a differentiated Gaussian pulse propagating in free space is used for absorption comparison of five different parameter settings. In addition, relative error for electric field is calculated for all PML types.

Comparison of sources utilization in FDTD, namely of a differentiated Gaussian pulse and a regular Gaussian pulse is given in Section 2. The numerical results clearly indicate the advantage of the differentiated Gaussian pulse. The basic theory and implementation of CPML in FDTD method is shown in Section 3. The numerical results and discussion presented in Section 4 suggest the criteria for the optimal CPML parameter setting strategy.

2. IMPULSIVE SOURCES

FDTD method allows modeling of the various electromagnetic propagation problems where the broad range of frequencies is included, by using just a single simulation. Therefore, it is generally suitable to use impulsive sources which can introduce a wide spectrum of frequencies rather than harmonic sources. The Gaussian pulse is a potentially convenient source and it is often used in this method. In time domain the Gaussian pulse is expressed as:

$$f(t) = e^{-\left(\frac{t-d}{w}\right)^2} \tag{1}$$

where t is time, d is a time delay and w is half-width of the Gaussian pulse. Besides its advantages, the Gaussian pulse contains DC (direct current) components, unwanted in FDTD modeling. Numerical reflections and unphysical fields are visible in the computational domain with sources containing DC components [18]. The shape of the Gaussian pulse in time and frequency domain, with d=0 and w=10, is presented in Fig 1.

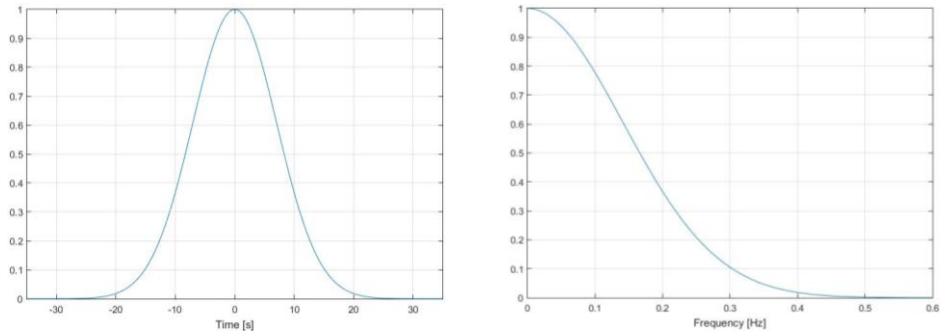

a) b)

Fig. 1. Gaussian pulse in: a) time domain; b) frequency domain

Besides the original Gaussian pulse, its first derivative in time:

$$f(t) = -2\left[\frac{(t-d)}{w}\right] e^{-\left[\frac{(t-d)}{w}\right]^2} \tag{2}$$

is commonly used in FDTD simulations, because it does not contain a DC component [19]. The time and frequency domain representation of the differentiated Gaussian pulse, with the same parameters as a regular Gaussian pulse, is shown in Fig. 2.

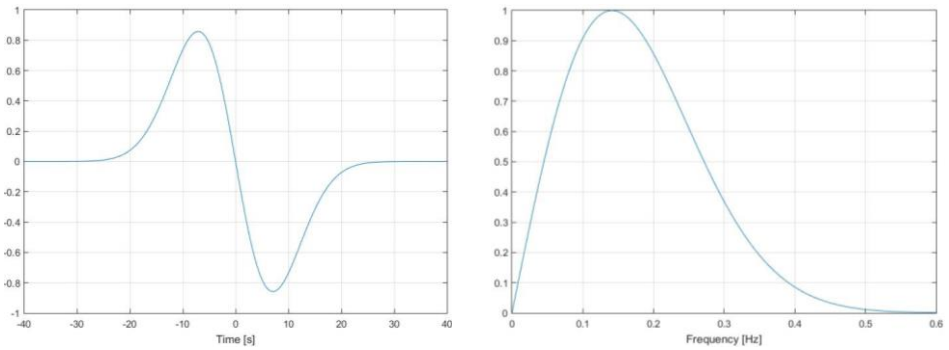

a) b)

Fig. 2. Differentiated Gaussian pulse in: a) time domain; b) frequency domain

In Fig. 3. the E_x field distribution of a Gaussian pulse and of a differentiated Gaussian pulse propagating in free space is presented. The computational domain's dimension is 100x80x100 space cells and electric field is presented in *xy* plane at 50th time-step. In Fig. 3(a), it can be clearly seen that the Gaussian pulse has an artificial DC component located at the center of the computational domain of the FDTD grid. These components are unphysical fields contributing to inaccurate analysis of numerical data. Otherwise, in Fig 3(b), in the differentiated Gaussian pulse simulation, there is no DC component in the center of the grid. Therefore, the use of a differentiated Gaussian pulse in the electromagnetic modeling of pulse sources in FDTD method is suggested. In all numerical experiments in this paper a differentiated Gaussian pulse is used as a source.

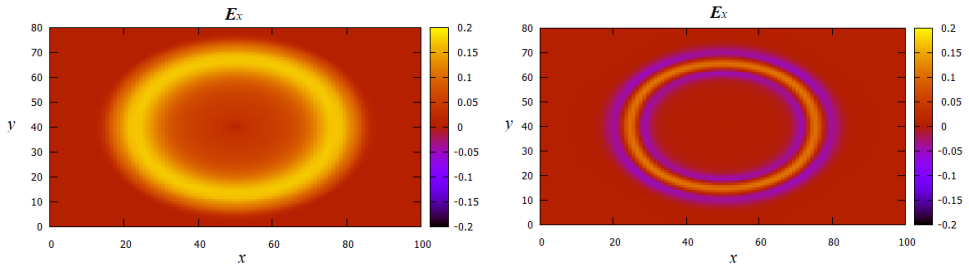

a) b)

Fig. 3. E_x field distribution of: a) Gaussian pulse; b) differentiated Gaussian pulse

3. CPML IMPLEMENTATION IN FDTD

Theoretically, all PML absorbing boundary conditions are based on an SC formulation of Maxwell's equation, with the main purpose of absorbing electromagnetic waves. CPML [12] is derived on the basis of the well-established Berenger's split-field PML [1] and unsplit form proposed in [2] (called UPML). CPML is based on complex frequency shifting (CFS) [9]. More precisely, the pole shifting of s_u (SC) into the upper–half of complex plane enabled mapping of Maxwell's equation into complex coordinate space with the PML parameters described as [9]:

$$s_u = k_u + \frac{\sigma_u}{\alpha_u + j\omega\varepsilon_0}\ , u=x,y,z, \tag{3}$$

where $k\geq 1$ is stretching coefficient, $\sigma\geq 0$ is medium conductivity, $\alpha\geq 0$ is complex frequency shift parameter and ε_0 is permittivity.

Stretched coordinates in the complex form of Ampere's law in free space are:

$$j\omega\varepsilon_0\vec{E} = \hat{x}\left(\frac{1}{s_y}\frac{\partial}{\partial y}\vec{H}_z - \frac{1}{s_z}\frac{\partial}{\partial z}\vec{H}_y\right) + \hat{y}\left(\frac{1}{s_z}\frac{\partial}{\partial z}\vec{H}_x - \frac{1}{s_x}\frac{\partial}{\partial x}\vec{H}_z\right) + \hat{z}\left(\frac{1}{s_x}\frac{\partial}{\partial x}\vec{H}_y - \frac{1}{s_y}\frac{\partial}{\partial y}\vec{H}_x\right) \tag{4}$$

and after time domain conversion:

$$\frac{\partial}{\partial t}\left(\varepsilon_0 \vec{E}\right)=\hat{x}\left(\bar{s}_y * \frac{\partial}{\partial y}\vec{H}_z-\bar{s}_z * \frac{\partial}{\partial z}\vec{H}_y\right)+\hat{y}\left(\bar{s}_z * \frac{\partial}{\partial z}\vec{H}_x-\bar{s}_x * \frac{\partial}{\partial x}\vec{H}_z\right)+\hat{z}\left(\bar{s}_x * \frac{\partial}{\partial x}\vec{H}_y-\bar{s}_y * \frac{\partial}{\partial y}\vec{H}_x\right) \quad (5)$$

where "*" represents convolution as a consequence of frequency dependence of SC metrics and $\bar{s}_u$ is the inverse Laplace transform of s_u^{-1}.

The Fourier transform of $\bar{s}_u$ is required, in order to derive CPML in time domain, hence:

$$\bar{s}_u(t)=F^{-1}\left(\frac{1}{k_u+\dfrac{\sigma_u}{\alpha_u+j\omega\varepsilon_0}}\right)=\frac{\delta(t)}{k_u}-\frac{\sigma_u}{\varepsilon_0 k_u^2}e^{-\left(\frac{\sigma_u}{\varepsilon_0 k_u}+\frac{\alpha_u}{\varepsilon_0}\right)}h(t)=\frac{\delta(t)}{k_u}+\eta(t) \quad (6)$$

where $\delta(t)$ is the unit impulse function, and $h(t)$ is the unit step function.

Implementing transformed $\bar{s}_u$ (6) in (3) yields convolution pairs on the right-hand side of the equation. The use of recursive convolution (RC) [11] technique avoids the usage of a huge amount of computer resources during the implementation in time domain. The discrete impulse response of convolution pairs and recursive convolution relation gives the expression:

$$\psi_{u,v}(n)=b_u\psi_{u,v}(n-1)+c_u\frac{\partial}{\partial u}H_v(n) \quad (7)$$

with:

$$b_u=e^{-\left(\frac{\sigma_u}{\varepsilon_0 k_u}+\frac{\alpha_u}{\varepsilon_0}\right)\Delta t}, \qquad c_u=\frac{\sigma_u}{k_u(\sigma_u+\alpha_u k_u)}[b_u-1] \quad (8)$$

In (8) coefficients are nonzero only in the PML region and computed with parameters σ_u, α_u and k_u (n=i,j,k; u=x,y,z). By implementing this form of $\Psi_{u,v}(n)$ good efficiency of time marching in the FDTD algorithm is achieved. Hence, FDTD time and space discretization of Ampere's law with CPML yields explicit update of $\vec{E}_x$ expressed as:

$$\vec{E}_x\Big|_{i+\frac{1}{2},j,k}^{n+\frac{1}{2}}=\frac{\left(1-\dfrac{\sigma_{i+\frac{1}{2},j,k}\Delta t}{2\varepsilon_{i+\frac{1}{2},j,k}}\right)}{\left(1+\dfrac{\sigma_{i+\frac{1}{2},j,k}\Delta t}{2\varepsilon_{i+\frac{1}{2},j,k}}\right)}\cdot\vec{E}_x\Big|_{i+\frac{1}{2},j,k}^{n-\frac{1}{2}}+\frac{\left(\dfrac{\Delta t}{\varepsilon_{i+\frac{1}{2},j,k}}\right)}{\left(1+\dfrac{\sigma_{i+\frac{1}{2},j,k}\Delta t}{2\varepsilon_{i+\frac{1}{2},j,k}}\right)}\cdot\left(\frac{\vec{H}_z\Big|_{i+\frac{1}{2},j+\frac{1}{2},k}^{n}-\vec{H}_z\Big|_{i+\frac{1}{2},j-\frac{1}{2},k}^{n}}{k_{y_j}\Delta y}-\frac{\vec{H}_y\Big|_{i+\frac{1}{2},j,k+\frac{1}{2}}^{n}-\vec{H}_y\Big|_{i+\frac{1}{2},j,k-\frac{1}{2}}^{n}}{k_{z_k}\Delta z}+\psi_{\vec{E}_{x,y}\Big|_{i+\frac{1}{2},j,k}^{n}}-\psi_{\vec{E}_{x,z}\Big|_{i+\frac{1}{2},j,k}^{n}}\right) \quad (9)$$

In (9) $\Psi_{Ex,y}$, $\Psi_{Ex,z}$ are PML coefficients which are defined only in the PML region. Similar expressions are derived for five remaining field components (E_y, E_z, H_x, H_y and H_z) for 3D FDTD domain, with the adequate replacement of (i,j,k) and (x,y,z).

Neither a split-field PML nor an SC PML represent a physical medium. It has been shown that PML and UPML have the same reflection properties [3, 4] causing large reflections at low frequencies [4-6].

The efficiency of CPML is mainly dependent on the proper choice of parameters. These pivotal parameters in all PML absorbing boundary conditions are summarized in Table 1.

Table 1 Key parameters affecting PML absorption

Parameters synthesis	Meaning	Effect in PML
$\boldsymbol{k}$	stretching coefficient	warping the space in order to attenuate the EM energy
$\boldsymbol{\sigma}$	conductivity	transform EM energy into heat energy
$\boldsymbol{\alpha}$	complex frequency shift parameter	determine the characteristic absorption frequency, suppress dispersion

The parameters from Table 1. can be spatially graded in different ways, but the most successful two are polynomial and geometric grading. In this paper, the polynomial grading is used. PML parameters are scaled as follows [12]:

$$k_u(n) = 1 + \left(\frac{n}{m}\right)^r (k_{u,\max} - 1), \tag{10}$$

$$\sigma_u(n) = \left(\frac{n}{m}\right)^r \sigma_{u,\max}, \tag{11}$$

$$\alpha_u(n) = \left(\frac{m-n}{m}\right)^{r_a} \alpha_{u,\max}, 0 \le n \le m. \tag{12}$$

where n is the PML loss depth, m is the PML thickness, r is exponential power and r_a is the scaling order. Conductivity σ_u is scaled to be 0 at the inner most PML layer (n=0) and $\sigma_{u,max}$ at the PML outer boundary (n=m). The stretching coefficient k_u is 1 at the inner surface of PML and $k_{u,max}$ at the outer most layer of PML. The complex frequency shift parameter α_u has a maximum at the inner most layer of PML, thereby decreasing the reflection error of evanescent modes. Inside the PML, α_u is decreased to a minimum in order to decay low frequencies of the wave propagating [12].

The CPML efficiency is strongly dependent on the proper setting of the CPML parameters. If $\sigma_{u,max}$ is too small, reflections from the outer CPML layers are dominant, while for large $\sigma_{u,max}$ induction fields on the inner most layers is inevitable [10]. An optimal relation for general media of polynomial graded $\sigma_{u,max}$ is proposed in [12]:

$$\sigma_{u,opt} = \frac{0.8(r+1)}{Z_0 \Delta_u \sqrt{\varepsilon_{r,eff}\,\mu_{r,eff}}}, \tag{13}$$

where Z_0 is the impedance of free space, Δ_u is spatial step in u=x,y,z direction, $\varepsilon_{r,eff}$ and $\mu_{r,eff}$ are effective relative permittivity and permeability, respectively.

In practice, implementation of CPML is simpler and more storage-efficient algorithm than PML and UPML [17]. Quite simple implementation of UPML in the existing FDTD codes, comes with the cost of doubling memory requirements through the entire FDTD domain. Complexity of programming is increased by the usage of triple-nested loops for the fields inside the computational domain, and with individual loops in UPML. Stored only in PML region of the FDTD algorithm, CPML variables are resulting in a better memory efficiency than UPML. Moreover, implementation of CPML remains the same in the case of lossy, dispersive, homogeneous and inhomogeneous mediums. Two additional variables per field component in all those mediums are required in the case of UPML [17].

4. Numerical Results and Discussions

A 3D FDTD simulation of electromagnetic wave propagation in free space with a differentiated Gaussian pulse as a source is used to analyze the CPML absorption efficiency. A relative error is calculated comparing absorption for different PMLs with different parameter settings.

The explicit FDTD algorithm is used and calculated by using the original C++ codes. The numerical results of the electromagnetic field and relative error graphs are plotted with the command-line driven *Gnuplot* graphing utility.

Dispersion analysis of PMLs with high-frequency impulsive source simulation

Numerous numerical experiments using the CPML algorithm in simulation of free space with high-frequency pulses are carried out and results are given in this section. A set of CPML parameters is taken from [12], and CPML-A and CPML-B serve to investigate the influence of k and α in the absorption of high-frequency electromagnetic waves generated from the pulse source.

The basic frequency of a differentiated Gaussian pulse is $f_{basic} \epsilon (0,3/w)$, where w is the base width of the Gaussian pulse [16]. The pulse energy has maximum for frequency $f=0$ and minimum for $f=3/w$. For the FDTD electromagnetic field simulations in this section, we set the pulse width w=30 ps, resulting in the frequency range of $f_{basic} \epsilon (0,100)$ GHz.

The propagation of a differentiated Gaussian pulse in free space in the 3D FDTD domain is simulated in 150x150x150 space lattice, with 1-mm-square cells and time-step of dt=1.906575 ps (0.99 times of CFL limit). The duration of the simulation is 600 time-steps (1.143945 ns). The high frequency differentiated Gaussian pulse (2) is placed in the centre of the computational domain with w=30 ps and d=4w. For comparison purposes, the 3D FDTD domain is terminated with 10-cell thick different PML-s: PML, UPML, CPML, CPML-A and CPML-B. The set of PML parameters used in the numerical experiments is listed in Table 2.

Given that all parameter settings share the same computational domain (free space), conductivity (σ_{max}), r = 3 and r_a = 1 [12], the reflected electromagnetic waves from the outer layers of PMLs will increase exponentially, but conductivity will suppress them equally.

Table 2. Set of parameters for different types of PMLs

Type of PML	k_{max}	σ_{max}	α_{max}
PML	1	$0.75\sigma_{opt}$	/
UPML	10	$0.75\sigma_{opt}$	/
CPML	20	$0.75\sigma_{opt}$	0.2
CPML-A	5	$0.75\sigma_{opt}$	9×10^{-4}
CPML-B	1	$0.75\sigma_{opt}$	3×10^{-4}

Fig. 4 displays snapshot aggregations of E_z (the z component in the electric field of differentiated Gaussian pulse) combining 5 groups of parameter settings and 3 moments. The xy plane of the snapshots is perpendicular to the z coordinate in a free space. The color bar indicates the values of E_z. The parameter settings for PML in Fig. 4 (a1-a3) are: k_{max} =1, σ_{max} = $0.75\sigma_{opt}$; the parameter settings for UPML in Fig. 4 (b1-b3) are: k_{max} =10, σ_{max} = $0.75\sigma_{opt}$; the parameter settings for CPML in Fig. 4 (c1-c3) are: k_{max} =20, σ_{max} = $0.75\sigma_{opt}$, α_{max} = 0.2; the parameter settings for CPML-A in Fig. 4 (d1-d3) are: k_{max} =5, σ_{max} = $0.75\sigma_{opt}$, α_{max} =9×10^{-4}; the parameter settings for CPML-B in Fig. 4 (e1-e3) are: k_{max} =1, σ_{max} = $0.75\sigma_{opt}$, α_{max} =3×10^{-4}. The parameter settings of PML and UPML show the absorption effect of high-frequency pulse with different k_{max} and without influence of α_{max}. The parameter settings of CPML, CPML-A and CPML-B show absorption for different k_{max} and α_{max}.

Figure 4 (a1-e1) presents the moment in time (200^{th} time-step) when pulse is propagated and electromagnetic waves just began to interact with the inner layers of PML. No reflection can be spotted in Fig. 4. (a1-e1), however some differences in absorption for different PMLs can be observed. For example, by comparing field plots in (a1) and (b1) in Fig. 4, it is clear that the waves are closer to the outer layers in (a1), which indicates that the propagation velocity is slower in (b1). Moreover, in (b1), the waves are absorbed before reaching the outer layers, but there is some reflection from the inside layers. Comparing (c1-e1) in Fig. 4, it can be seen that in (c1), the waves did not reach the outer layers also and small reflection began to rise. For (d1) and (e1), the waves are linearly absorbed without reaching the outer layers. Considering that in (b1) (UPML) and (c1) (CPML) parameter k_{max} is 10 and 20, respectfully, it is reasonable to conclude that increasing k_{max} will decrease the propagation velocity of the electromagnetic wave.

In the next time-step (230^{th}) shown in Fig. 4 (a2-e2), all the wave fronts reached the outer layers. Hence, different absorption of the wave fronts can now be noticed. In Fig. 4 (a2-b2), the waveform is slightly distorted, following the significant amount of dispersion. The smaller dispersion can be seen in Fig. 4 (c2). Moreover, the waves are absorbed by the CPML-A and CPML-B for the most part, in Fig. 4 (d2-e2). Since the parameter α_{max} is not defined in PML and UPML, and in CPML α_{max} equals 0.2, it is clear that existence of α_{max} considerably affects the absorption of electromagnetic waves. Considering that α_{max} and k_{max} are much smaller in CPML-A and CPML-B than in CPML, the reasonable conclusion is that the absorption in PMLs is not only dependent on the values of the parameter as much as of its ratio.

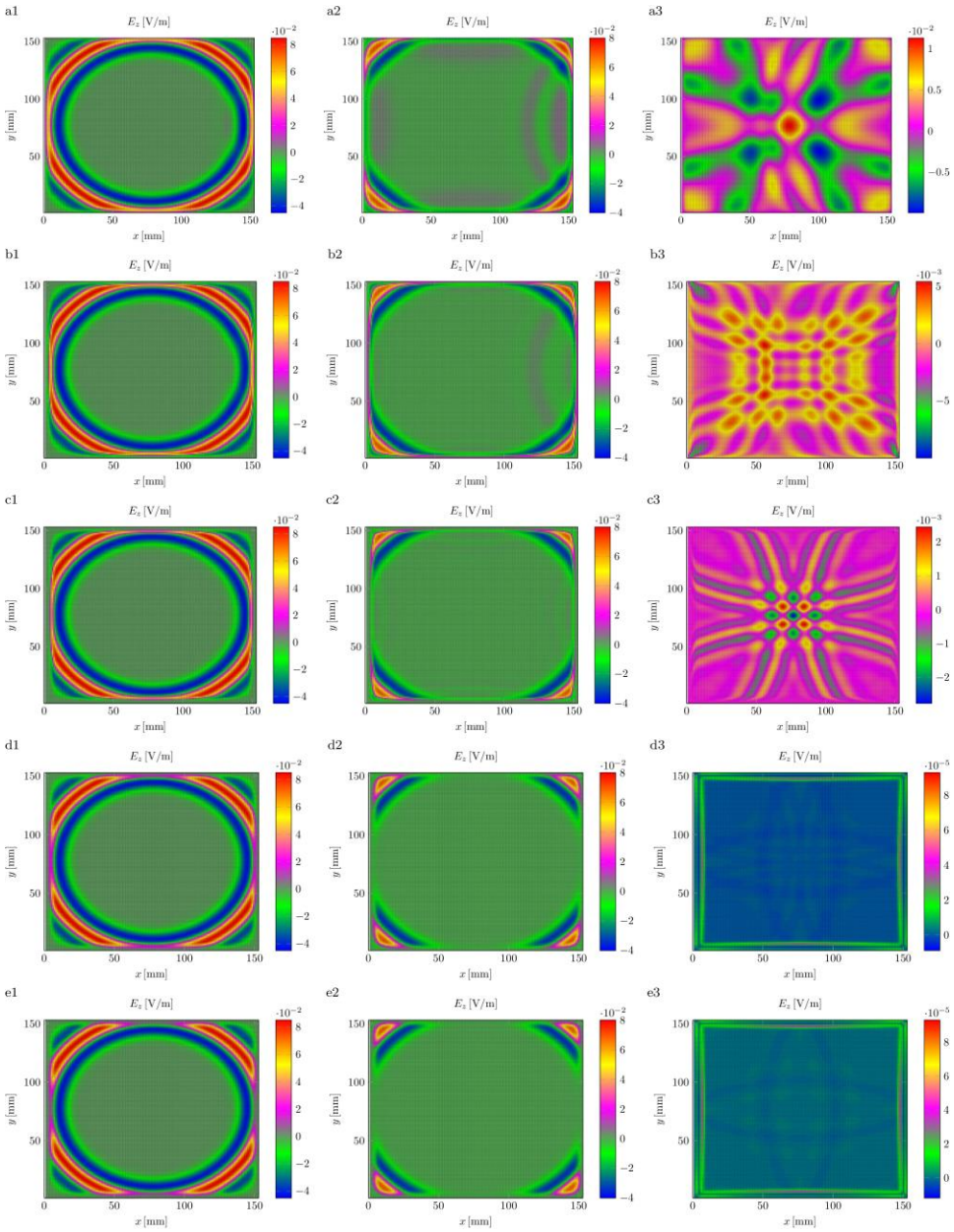

Fig. 4 Snapshots of absorption effects for different types of PML. E_z field component distribution in *xy* plane. With all other parameter remain constant, the parameter settings of (a1) to (a3) is PML; (b1) to (b3) is UPML; (c1) to (c3) is CPML; (d1) to (d3) is CPML-A; (e1) to (e3) is CPML-B. The time of (a1) to (e1) is 200th time-step; (a2) to (e2) is 230th time-step; (a3) to (e3) is 300th time-step.

Fig 4. (a3-e3) presents the dispersion for different PML parameter settings at 300th time-step of the simulation. When we compare Fig. 4 (a3), (b3) and (c3), we can see that the absorption is poor in Fig. 4 (a3) and (b3). The results from (c3) and parameter settings of PML, UPML and CPML, lead to conclusion that the influence of the parameter α_{max} has a significant contribution in absorption as it had in the previous time-step. On the other side, in Fig. 4 (d3) and (e3), there is a very low dispersion even though the parameter α_{max} is much smaller than in (c3). Therefore, the dispersion is positively correlated with the increase of the parameter k_{max} and the absorption has to be precisely controlled with the choice of the parameter α_{max}. Although k_{max} is bigger in (d3) than in (e3), there is a better absorption in (d3). That is because the parameter α_{max} is bigger in (d3) than in (e3), therefore, larger α_{max} enables CPML to possess a higher absorption capability. From Fig. 4 (d3) it is clear that larger k_{max} makes the electromagnetic waves velocity lower, so that α_{max} dominantly affects the absorption from artificial PML boundaries.

The relative error is calculated for electric field E at point B, in order to examine absorption characteristics with different PML parameter settings, as shown in Fig. 5. The test domain with 40 x 40 x 40 cell grid and the reference domain with 400 x 400 x 400 cell grid are used for relative error calculation, defined as:

$$R\Big|_{i,j,k}^{n} = 20\log_{10}\frac{\left|\vec{E}\Big|_{i,j,k}^{n} - \vec{E}_{ref}\Big|_{i,j,k}^{n}\right|}{\left|\vec{E}_{ref\,\max}\Big|_{i,j,k}\right|}. \tag{14}$$

In (19), $E\big|_{i,j,k}^{n}$ is the electric field at probe point and time-step n in the test domain, $E_{ref}\big|_{i,j,k}^{n}$ is the electric field at probe point and time-step n in the reference domain and $E_{ref\,\max}\big|_{i,j,k}^{n}$ is the maximum amplitude of the reference field at probe point over the time-stepping range of interest. The reference domain is kept sufficiently large to avoid reflection from the walls of FDTD domain during 1000 time-steps of interest. The same source function as for differentiated Gaussian pulse propagation in free space is used, with w = 30 ps, d = 4w, in test and reference domain. An identical source location (centered in FDTD grid) is used for both domains and probe points are at the same position relative to the source. Point B (38,20,38) in test domain correspond to point B (218,200,218) in the reference domain.

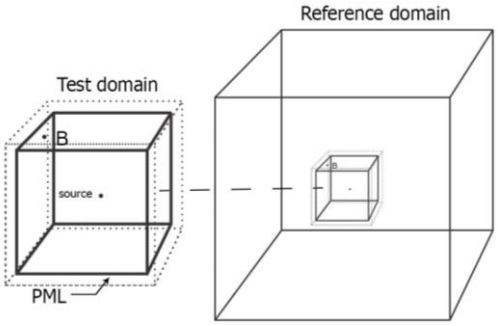

Fig. 5 Test and reference FDTD domain illustration used for calculation of relative error

The relative error for calculated all three E field components at point B in the case of 10-cell thick PMLs is shown in Fig. 6. Parameter settings for PML, UPML, CPML,

CPML-A and CPML-B are from Table 2. The early time error peaks, due to discretization error, can be observed in Fig. 6, which slowly decay after the time-stepping increase. Comparing the PML and UPML graphs it is noticeable that UPML provides some error reduction, as the consequence of the parameter k_{max} increasing. The CPML graph shows fine absorption of electromagnetic waves in comparison with PML and UPML. Although the absorption is much better in CPML, the late time dispersion (from 760th to 920th time-step) is a consequence of reflected waves induced by the increased k_{max}.

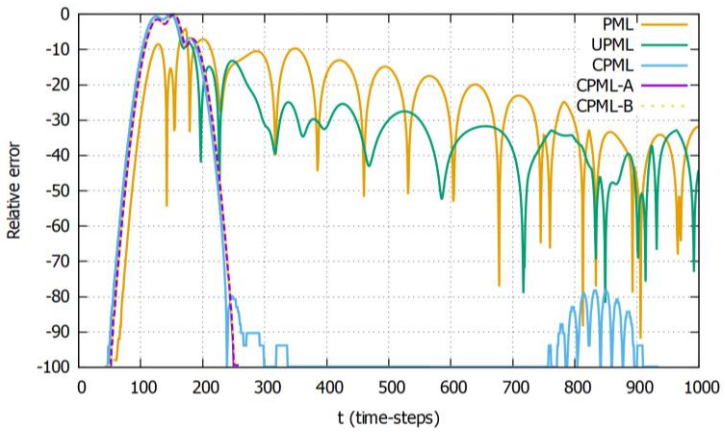

Fig. 6. Relative error for 10 cell-thick different types of PML changing over time.

In Fig. 6, CPML-A and CPML-B graphs show the same error due to almost the same parameter settings. Error reduction is significantly higher in comparison with PML, UPML and CPML graphs. There is no late time dispersion as well. Considering the results from Fig. 4 (d3-e3) and graphs from Fig. 6, it is clear that the optimal parameter settings should be in range of the CPML-A and CPML-B parameters.

Overall, the choice of k_{max} is decisive for both the absorption efficiency and dispersion, because of the evident positive dependence between them. When the FDTD method is used for modelling electromagnetic wave propagations in the presence of high frequency electromagnetic source, the inevitable skin-effect cannot be neglected. In such cases, setting the absorption efficiency of the CPML to depend more on σ and α_{max} and adjusting k_{max} sufficiently small will result in a negligibledispersion.

5. CONCLUSION

Five different CPML parameter settings are used in the high-frequency impulsive source FDTD simulation in order to improve the absorption mechanisms of CPML. We simulated free space propagation of a differentiated Gaussian pulse in the 3D FDTD computational domain. The calculated absorption led us to an optimal CPML parameter setting in our research. The results indicate that the larger values of the stretching coefficient will increase both the absorption and dispersion. However, for complete suppression of dispersion, the stretching coefficient should be kept equal to 1. Therefore, the absorption should be controlled with the complex frequency shift parameter and conductivity.

REFERENCES

[1] J. P. Berenger, "A perfectly matched layer for the absorption of electromagnetic waves", Journal of Computational Physics, vol.114, pp.185200, *1994.* [Online]. Available: https://doi.org/10.1006/jcph.1994.1159

[2] Z. S. Sacks, D. M. Kingsland, R. Lee, J. F. Lee, "A perfectly matched anisotropic absorber for use as an absorbing boundary condition", IEEE Trans. Antennas Propagat., vol. 43, pp. 1460–1463, 1995. [Online]. Available: https://doi.org/10.1109/8.477075

[3] J. P. Berenger, "Numerical reflection from FDTD PMLs: A comparison of the split PML with the unsplit and CFS PMLs", IEEE Trans. Antennas Propagat., vol. 50, p. 258–265, 2002. [Online]. Available: https://doi.org/10.1109/8.999615

[4] D. Correia, J. M. Jin, "Performance of regular PML, CFS-PML, and Second-order PML for waveguide problems", Microwave andOptical Technology Letters, vol. 48, pp. 2121–2126, 2006. [Online]. Available: http://onlinelibrary.wiley.com/doi/10.1002/mop.21872/full

[5] W. C. Chew, W. H. Weedon, "A 3D perfectly matched medium from modified Maxwell's equations with stretched coordinates", IEEE Microwave Guided Wave Lett., vol. 7, pp. 599–604, 1994. [Online]. Available: http://onlinelibrary.wiley.com/doi/10.1002/mop.4650071304/full

[6] C. M. Rappaport, "Perfectly matched absorbing boundary conditions based on anisotropic lossy mapping of space", IEEE Microwave Guided Wave Lett., vol. 5, pp. 90–92, 1995. [Online]. Available: https://doi.org/10.1109/75.366463

[7] F. L. Teixeira, W. C. Chew, "PML-FDTD in cylindrical and spherical coordinates", IEEE Microwave Guided Wave Lett., vol. 7, pp. 285–287, 1997. [Online]. Available: https://doi.org/10.1109/75.622542

[8] F. L. Teixeira, K. P. Hwang, W. C. Chew, J. M. Jin, "Conformal PML-FDTD schemes for electromagnetic field simulations: A dynamic stability study", IEEE Trans. Antennas Propagat., vol. 49, pp. 902–907, 2001. [Online]. Available: https://doi.org/10.1109/8.931147

[9] M. Kuzuoglu, R. Mitra, "Frequency dependence of the constitutive parameters of causal perfectly matched anisotropic absorbers", IEEE Microwave Guided Wave Lett., vol. 6, pp. 447–449, 1996. [Online]. Available: https://doi.org/10.1109/75.544545

[10] J. P. Berenger, "An optimized CFS-PML for Wave-Structure Interaction Problems", IEEE Transactions on Electromagnetic Compatibility, vol. 54, pp. 351–358, 2012. [Online]. Available: https://doi.org/10.1109/TEMC.2011.2178852

[11] R. J. Luebbers, F. Hunsberger, "FDTD for Nth-order dispersive media", IEEE Trans. Antennas Propagat., vol. 40, pp. 1297–1301, 1992. [Online]. Available: https://doi.org/10.1109/8.202707

[12] J. A. Roden, S. D. Gedney, "Convolutional PML (CPML): An efficient FDTD implementation of the CFS-PML for arbitrary media", Microwave Optical Tech. Lett., vol. 27, pp. 334–339, 2000. [Online]. Available:http://onlinelibrary.wiley.com/doi/10.1002/10982760(20001205)27:5%3C334::AIDMOP1%3E3.0.CO;2-A/full

[13] I. Giannakis, A. Giannopoulos, "Time-Synchronized Convolutional Perfectly Matched Layer for Improved Absorbing Performance in FDTD", IEEE Antennas and Wireless Propagation Letters, vol. 14, pp. 690–693, 2015. [Online]. Available: https://doi.org/10.1109/LAWP.2014.2376981

[14] P. Lee, J. L. Vay, "Efficiency of the Perfectly Matched Layer with high-order finite difference and pseudo-spectral Maxwell solvers". Computer Physics Communications, vol. 194, pp. 1–9, 2015. [Online]. Available: https://doi.org/10.1016/j.cpc.2015.04.004

[15] Z. H. Li, Q. H. Huang, "Application of the complex frequency shifed perfectly matched layer absorbing boundary conditionsin transient electromagnetic method modelling", Chinese J. Geophys, vol. 57, pp. 12921299,2014.[Online].Available:http://en.cnki.com.cn/Article_en/CJFDTOTALDQWX201404026.htm

[16] Fang, Sinan, et al. "Crosswell electromagnetic modeling from impulsive source: Optimization strategy for dispersion suppression in convolutional perfectly matched layer." Scientific reports, vol. 6, 2016. [Online]. Available: https://dx.doi.org/10.1038%2Fsrep32613

[17] B. D. Gvozdic, D. Z. Djurdjevic, "Performance advantages of CPML over UPML absorbing boundary conditions in FDTD algorithm.", Journal of Electrical Engineering, vol. 68, no 1, pp. 47-53, 2017. [Online]:http://iris.elf.stuba.sk/JEEEC/data/pdf/1_117-06.pdf

[18] Wenhua Yu, *Electromagnetic simulation techniques based on the FDTD method*, Vol. 221, John Wiley & Sons, 2009.

[19] Umran S. Inan, Robert A. Marshall, *Numerical electromagnetics: the FDTD method*, Cambridge University Press, 2011.